Chinese Chemical Letters 33 (2022) 4043–4047

Contents lists available at ScienceDirect

Chinese Chemical Letters

journal homepage: www.elsevier.com/locate/cclet

Study of a water-soluble supramolecular complex of curcumin and β-cyclodextrin polymer with electrochemical property and potential anti-cancer activity

Wang Zhang[a,1,*], Ping Xiao[a,1], Liwei Lin[b,1], Fang Guo[a], Qingyue Wang[c], Yuanzhe Piao[b,d,*], Guowang Diao[a,*]

[a] School of Chemistry and Chemical Engineering, Yangzhou University, Yangzhou 225002, China
[b] Department of Applied Bioengineering, Graduate School of Convergence Science and Technology, Seoul National University, Suwon 443-270, Republic of Korea
[c] Shanghai Suni Biotechnology Development Co., Ltd., Shanghai 201300, China
[d] Advanced Institutes of Convergence Technology, Suwon 443-270, Republic of Korea

ARTICLE INFO

Article history:
Received 14 September 2021
Revised 9 December 2021
Accepted 14 December 2021
Available online 20 December 2021

Keywords:
Cyclodextrin polymer
Curcumin
Solubility
Anti-cancer activity
Supramolecular complex

ABSTRACT

As a member of the curcuminoid compound family, curcumin (Cur) has many interesting therapeutic properties. However, its low aqueous solubility and stability have resulted in poor bioavailability and restricted clinical efficacy. Based on size matching, β-cyclodextrin polymer (β-CDP), with its hydrophilic polymer chains and hydrophobic cavities, can form an inclusion complex with Cur. To improve the water solubility and stability of Cur, a simple and eco-friendly grinding method was designed to form β-CDP inclusion complexes. According to the Boltzmann–Hamel's method and Job's method, the molar ratio of the β-CD unit in β-CDP to Cur was determined to be 1:1. The diffusion coefficient and diffusion activation energy of Cur-β-CDP were calculated in an electrochemical study. This supramolecular complex worked well *in vitro* to inhibit the proliferation of hepatoma carcinoma cells HepG2. Remarkably, this method visibly reduced the undesirable side effects on normal cells, without weakening the anti-cancer activity of the drugs. We expect that the obtained host–guest complex will provide a new approach for delivering natural drug molecules, having low water solubility.

Curcumin (Cur) is an orange polyphenol that is extracted from the rhizome of perennial plants in the Zingiberaceae family [1]. The polyphenol structure, containing an unsaturated carbonyl scaffold, provides Cur with various therapeutic properties, such as being antioxidant, anti-inflammatory and antineoplastic. These properties have a wide range of applications in daily life, including use as anti-inflammatory drugs [2–4], antioxidants [5–7], food coloring agents [8], and so on [9–11]. In addition, Cur has been shown to control the growth and propagation of many types of tumor cells [12–14]. Mehrgan's group synthetized Cur–silica nanoparticles as photosensitizers for the photodynamic treatment of human melanoma cancer cells, to improve their application in cancer treatment [15]. Notably, Cur inhibits cell proliferation and promotes cell breakdown; it has been also shown to have effective therapeutic values [8]. However, Cur has restricted applications owing to its low bioavailability, poor water solubility, and rapid metabolism [16]. To solve these problems, we employed the supramolecular host compound, β-cyclodextrin polymer (β-CDP).

Cyclodextrins (CDs), as 2nd-generation supramolecular host compounds, typically contain 6–12 D-glucosamine units [17]. They possess a hollow circular truncated cone structure with a hydrophobic inner cavity and hydrophilic outer surface. CDs can accommodate various guest molecules in their cavities, to form stable host–guest inclusion complexes [18,19]. Owing to its low cost, nontoxic nature, and pro-environment properties, CD is widely used in food [20,21], medicine [22,23], agriculture [24] and other fields [25,26]. Recently, β-CDPs have received widespread attention as they show better water solubility and a higher inclusion efficiency than the parent β-CD [27,28]. Inclusion complexes with β-CDP can be prepared via several techniques such as co-precipitation, kneading, slurry complexation, spray drying, and freeze drying techniques [29]. Compared with CD, CDPs with dis-

* Corresponding authors.
E-mail addresses: zhangwang@yzu.edu.cn (W. Zhang), parkat9@snu.ac.kr (Y. Piao), gwdiao@yzu.edu.cn (G. Diao).
[1] These authors devoted equally to this work and should be considered as co-first authors.

https://doi.org/10.1016/j.cclet.2021.12.037
1001-8417/

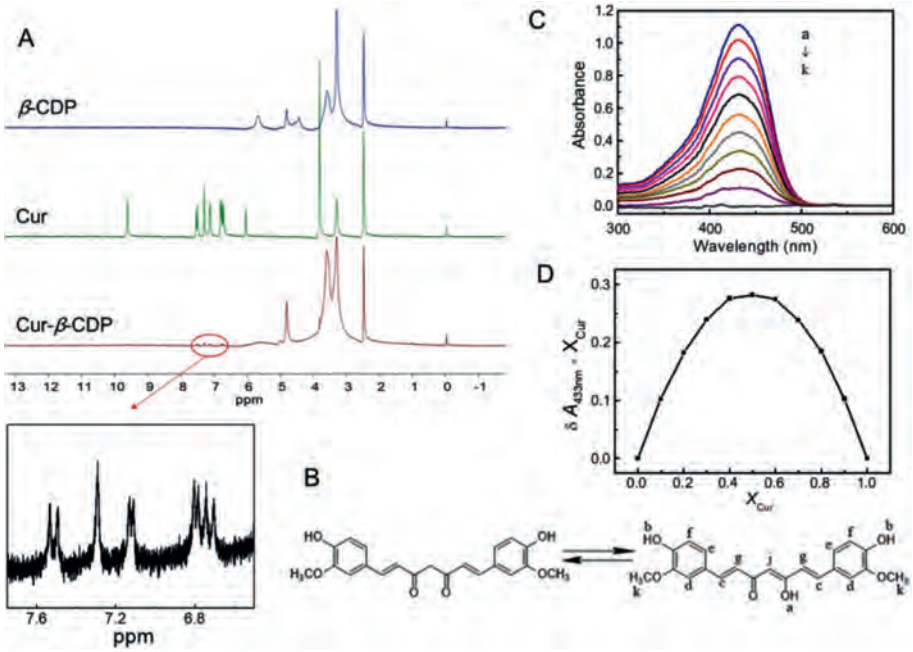

Fig. 1. (A) The ^{1}H NMR of Cur, Cur-β-CDP and β-CDP. (B) The potential solution structures of Cur. (C) UV–vis absorption spectra of Cur and β-CDP different molar ratios in water/ethanol mixed solution (V_{water}:$V_{ethanol}$ = 1:1) with a constant concentration of [β-CDP]+[Cur] = 40 μmol/L: (a) [Cur] = 40 μmol/L; (b) β-CDP:[Cur] = 1:9; (c) β-CDP:[Cur] = 2:8; (d) [β-CDP]:[Cur] = 3:7; (e) [β-CDP]:[Cur] = 4:6; (f) [β-CDP]:[Cur] = 5:5; (g) [β-CDP]:[Cur] = 6:4; (h) [β-CDP]:[Cur] = 7:3; (i) [β-CDP]:[Cur] = 8:2; (j) [β-CDP]:[Cur] = 9:1; (k) [β-CDP] = 40 μmol/L. (D) Job plot showing the 1:1 binding stoichiometry of the complex between β-CDP and Cur by plotting the difference in absorption at 433 nm against the mole fraction of Cur at an invariant total concentration of Cur in solution.

tinct physical and chemical properties have been widely exploited for solubilization and pharmaceuticals [30–32].

In this study, the Cur-β-CDP was prepared following a grinding method as shown in Fig. S1A (Supporting information), and the complex was evaluated using and the complex was evaluated using Fourier transform infrared (FT-IR), ultraviolet (UV), and nuclear magnetic resonance (NMR) spectroscopies. In Figs. S1B and C (Supporting information), Cur-β-CDP dispersed more easily in aqueous solution as compared to pure Cur. The aqueous inclusion complex solution was yellowish green, uniform, and stable, indicating that β-CDP could form water-soluble inclusion complexes with Cur. The improving water solubility of Cur-β-CDP allowed for the electrochemical analysis of Cur-β-CDP in the aqueous phase. In addition, we conducted an *in vitro* cytotoxicity study of β-CDP. The Cur-β-CDP in aqueous solutions was expected to enhance hydrophilicity and bioavailability of Cur.

The formation of the Cur-β-CDP inclusion complex was determined using FT-IR spectroscopy. Fig. S2 (Supporting information) shows the FT-IR spectra of β-CDP, Cur and the inclusion complex. The peaks for β-CDP were observed at 3394, 2929 and 1032 cm^{-1}, which were assigned to the stretching vibration of –OH, the anisotropic stretching vibration of –CH_2, and the stretching vibration of C–O–C, respectively [33]. The FT-IR spectrum of Cur showed an absorption peak at 3505 cm^{-1}, indicating the stretching vibration of the phenolic O–H [34]. In addition, the red line shows the bending vibration of the olefinic C–H of Cur at 1429 cm^{-1} and the aromatic C–O stretching vibration of Cur at 1278 cm^{-1}. The characteristic peaks at 1598 (stretching vibration of the benzene ring of Cur) and 1510 cm^{-1} (C–O and C–C vibrations of Cur) are shown in Fig. S2 (Supporting information). In the FT-IR spectrum of Cur-β-CDP, the characteristic peaks of Cur (as the guest molecule) nearly disappeared, while the peaks of β-CDP (as the host molecule) are retained owing to the host–guest interaction. Because of the shielding effect, only weak phenolic O–H and C–O vibrations at 1589 and 1517 cm^{-1} were observed, suggested that Cur molecules entered the hydrophobic cavities of β-CDP. This resulted in a significant decrease in the infrared absorption peaks for Cur. Thus, the results indicated the formation of Cur-β-CDP.

As shown in Fig. 1A, the dimensional accommodations of Cur, Cur-β-CDP, and β-CDP were studied *via* ^{1}H NMR spectroscopy. Cur usually exists in an enol form (Fig. 1B) in DMSO–d_6 solvents [35,36]. The ^{1}H NMR spectra of Cur and β-CDP were consistent with those reported in the literatures [35,37]. When host–guest interactions occur, the modification of the physical and chemical environment affects the atoms of Cur and β-CDP, which should result in changes in their chemical shifts [38]. The ^{1}H NMR spectra were obtained to confirm the formation of Cur-β-CDP. In the ^{1}H NMR spectra of Cur-β-CDP, all β-CDP peaks were observed after the formation of the inclusion complex [39]. However, their signals were slightly shifted owing to the host–guest interactions with Cur, as listed in Table S1 (Supporting information). In addition, the chemical shifts of protons H_c and H_g of Cur changed from 7.57–6.78 ppm to 7.56–6.77 ppm, respectively. According to reports by Wimmer *et al.* [40], Cur is an aliphatic guest complex, having a low association constant, that usually shows insignificant chemical shifts. This is similar to the above small chemical shifts seen in the CD complexes. Furthermore, the peaks for the Cur aromatic rings, ascribed from 6.40 ppm to 7.70 ppm after the inclusion complex formation, were significantly weakened compared with the ^{1}H NMR spectra of Cur in Fig. 1A. This indicates that the aromatic rings of Cur were placed inside the CD cavities. Thus, the above results indicate that Cur and β-CDP form inclusion complexes via supramolecular interactions.

As shown in Fig. S3 (Supporting information), the Cur-β-CDP inclusion complex was also investigated using thermogravimetric analysis (TGA). From 139 °C to 400 °C, the mass loss of Cur approached nearly 60%, while the mass loss of Cur-β-CDP decreased between 299 °C to 398 °C. The decomposition temperature of Cur-β-CDP was higher than that of Cur and close to that of β-CDP. This result was indicative of the formation of the Cur-β-CDP complex,

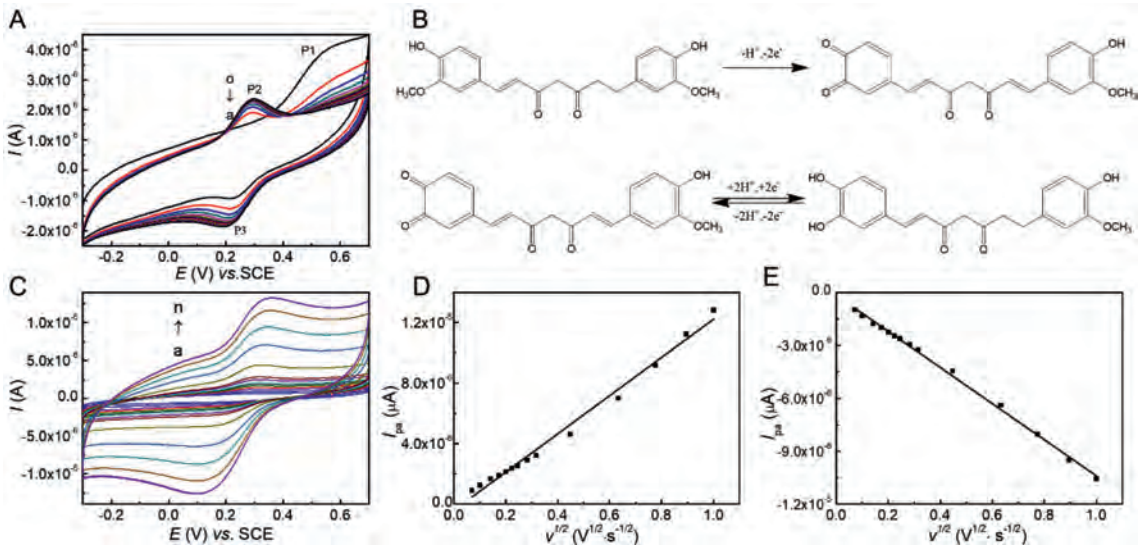

Fig. 2. (A) At 25 °C, the cyclic voltammograms of 1.0 mmol/L Cur-β-CDP in 0.1 mol/L PBS (pH 6.0) over fifteen consecutive cycles at a bare GCE at the scan rate of 50 mV/s at room temperature: (a) 1; (b) 2; (c) 3; (d) 4; (e) 5; (f) 6; (g) 7; (h) 8; (i) 9; (j) 10; (k) 11; (l) 12; (m) 13; (n) 14; (o) 15. (B) The electrochemical electrode reaction equation of Cur. (C) At 25 °C, the cyclic voltammograms of 1.0 mmol/L Cur-β-CDP in 0.1 mol/L PBS (pH 6.0) at different scan rate (mV/s): (a) 5; (b) 10; (c) 20; (d) 30; (e) 40; (f) 50; (g) 60; (h) 80; (i) 100; (j) 200; (k) 400; (1) 600; (m) 800; (n) 1000. The plot of (D) I_{pa} and (E) I_{pc} *vs.* $v^{1/2}$. Data were taken from (C).

which improves the thermal stability of Cur. The mass fraction of Cur in the inclusion complex was calculated to be approximately 20.2% based on the TGA results.

To study the host–guest interaction between Cur and β-CDP, a mixed solvent (ethanol and water, $V_{ethanol}$:V_{water} = 1:1) was chosen. Fig. S4A (Supporting information) shows the UV–vis spectra of a 1.0 × 10^{-5} mol/L Cur solution with differing concentrations of β-CD unit in β-CDP at 25 °C. It was found that the peak position of Cur at 433 nm did not change with the addition of β-CDP. However, the peak intensity increased with increasing β-CDP content. If the mole ratio of Cur to the CD structural unit of β-CDP in the inclusion complex is assumed to be 1:1, the following equation can be used to calculate the dissociation constant of the inclusion complex [41]:

$$\frac{[H]_0[G]_0}{\Delta A}=\frac{[H]_0}{\Delta\varepsilon}+\frac{k_D}{\Delta\varepsilon} \quad (1)$$

where H represents the host (CD unit in β-CDP), G is the guest (Cur), and HG is the inclusion complex (Cur-β-CDP). The initial concentrations of H and G were $[H]_0$ and $[G]_0$, respectively, where $[H]_0 \gg [G]_0$. ΔA is the change in absorbance, and $\Delta\varepsilon$ is the change in molar absorption coefficient. K_D is the dissociation constant of the inclusion complex.

A straight line was obtained by plotting $([H]_0[G]_0)/\Delta A$ *versus* $[H]_0$, as shown in Fig. S4B (Supporting information). The good linear relationship (R^2 = 0.990) proved that the assumption of a 1:1 molar ratio of Cur and β-CD units in β-CDP was correct. According to the slope and intercept of the straight line, the dissociation constant K_D of the inclusion complex was determined to be 6.4 × 10^{-3} mol/L. Compared with the inclusion complex of Cur and β-CD [42], the larger diffusion coefficient of Cur-β-CDP suggested that β-CDP could form a Cur inclusion complex more easily than β-CD. The result shows that the polymer chain has stronger intermolecular interactions than β-CD, inducing the formation of inclusion complexes more effectively [43].

The stoichiometry of the inclusion complex was also confirmed using the continuous variation of Job's method using UV–vis spectroscopy [44]. In the UV–vis absorption spectra of Cur and β-CDP in water/ethanol (V_{water}:$V_{ethanol}$ = 1:1), the sum of the concentrations of both components remained constant. The Job's plot of the complex formed between Cur and the β-CD units in β-CDP is shown in Figs. 1C and D, confirming the formation of a 1:1 inclusion complex between Cur and the β-CD unit in β-CDP. The complexation between β-CDP and Cur was also demonstrated by fluorescence spectrometer. Compared with the fluorescence spectra of Cur-β-CDP and Cur, the peak attributed to Cur in the inclusion complex showed a blue shift (Fig. S5 in Supporting information). It can be seen from the fluorescence spectra that the polarizability of Cur might be influenced when it was encapsulated in the hydrophobic cavity of CDP.

Fig. 2A displays the multi-cyclic voltammograms of 1.0 × 10^{-6} mol/L Cur-β-CDP in 0.1 mol/L PBS (pH 6.0) at 25 °C with a scan rate of 50 mV/s over 15 consecutive cycles on a bare GCE. In the first cyclic scan, Cur-β-CDP showed an oxidation peak (P1) at 0.544 V and reduction peak (P2) at 0.251 V. In the second cycle, a new oxidation peak (P3) at 0.299 V formed in place of P1. However, virtually no change was observed in P2. After two cycles, only P2 and P3 were observed. This revealed that P1 was an irreversible oxidation peak, and that P2 and P3 were redox peaks, where the active group came from the product of the first irreversible cycle. This is similar to the electrochemical electrode reaction of Cur [45]. The Cur structure contains two phenol rings that are substituted with two hydroxyl groups and two methoxy groups, which are involved in the electrochemical reactions of Cur-β-CDP. The electrochemical electrode reaction is shown in Fig. 2B. In the first cycle, the Cur in the CD cavity loses one proton and two electrons, resulting in a transition to an active intermediate state. In the second cycle, a reversible redox reaction of the active intermediate may involve the transfer of two electrons and two protons [46]. The supramolecular interaction between Cur and β-CDP has little effect on the good electrochemical redox capacity of Cur, while it is in the CD cavity. Moreover, the high solubility of Cur-β-CDP drives more Cur to participate in the electrochemical process. The good electrochemical activity of Cur-β-CDP was taken advantage of in a potential analytical application for determining Cur.

The cyclic voltammograms of 1.0 mmol/L Cur-β-CDP in 0.1 mol/L PBS (pH 6.0) at 25 °C with various scan rates are shown in Fig. 2C. The peak current (i_p) was calculated according to the Randles–Sevick equation [31].

$$i_P=-\left(2.69\times10^5\right)n^{3/2}Ac^*D^{1/2}v^{1/2} \quad (2)$$

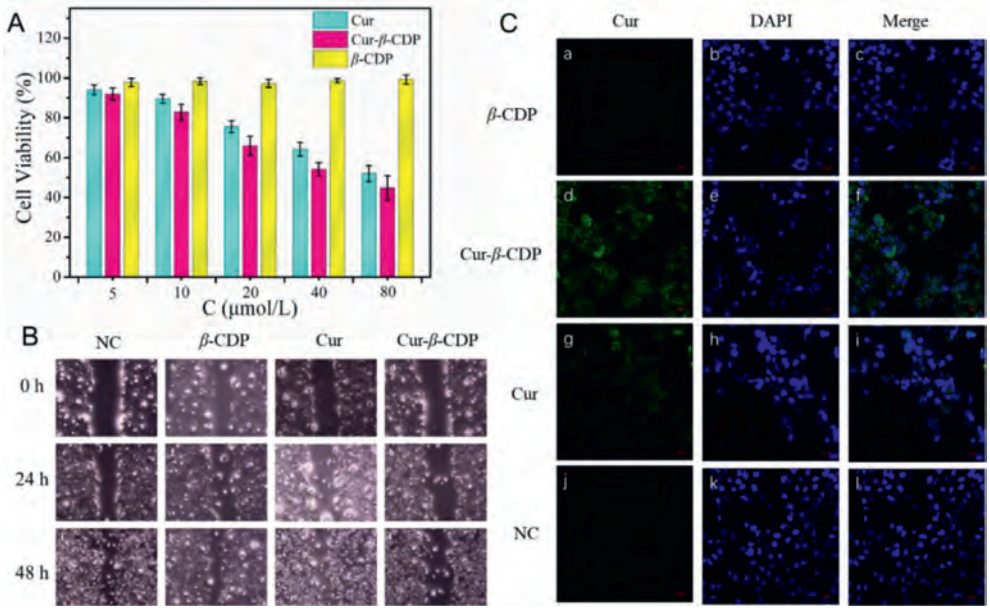

Fig. 3. (A) The cell viability of different concentration of Cur, Cur unit in Cur-β-CDP and β-CD unit in β-CDP. (B) The effect of Cur, β-CDP and Cur-β-CDP on migration in HepG2 cells, the images of HepG2 cells treated with Cur, β-CDP and Cur-β-CDP for 0, 24, 48 h after scratching were captured, respectively. (C) Confocal images of Hepg2 cells incubated with Cur, β-CDP and Cur-β-CDP for 24 h.

where n ($n = 2$) is the number of electrons transferred for the electrochemical reaction, A is the geometric surface area of the electrode, and c is the total concentration of Cur in the inclusion complex.

As shown in Figs. 2D and E, the redox peak currents of Cur-β-CDP were directly proportional to the square root of the scan rate in the range of 0.005–1.000 V/s in PBS (pH 6.0). It was demonstrated that the linear relationship ($R^2 = 0.990$ and $R^2 = 0.997$) corresponds to the peak anode current $i_{pa} \sim \nu^{\frac{1}{2}}$ and peak cathode current $i_{pc} \sim \nu^{\frac{1}{2}}$, respectively. This indicates that the electrochemical redox process of Cur-β-CDP is a *quasi*-reversible and diffusion-controlled process under the experimental conditions. At most sweep speeds, the value of i_{pa}/i_{pc} was close to 1 (theoretically $i_{pa}/i_{pc} = 1$). The electron transfer of Cur on the electrode surface was prohibited because of the shielding effect of β-CDP, and i_{pa} was slightly less than i_{pc}. For a *quasi*-reversible electrode process, the estimation of the diffusion coefficients of the oxidation state (D_O) and reduction state (D_R) could be determined from the slope of the Randles–Sevcik plot using Eq. 2. D_O and D_R were calculated as 7.94×10^{-8} and 9.91×10^{8} cm^2/s, respectively.

The cyclic voltammograms of Cur-β-CDP in 0.1 mol/L PBS (pH 6.0) at different temperatures are shown in Fig. S6A (Supporting information). It clearly shows that the peak current i_p and peak potential E_p were affected by the temperature. When the temperature increased, E_p moved in a negative direction, and i_p increased. By using Eq. 3, the diffusion coefficient of Cur-β-CDP at a series of temperatures can be obtained. The linear fitting relationship between the diffusion coefficient D and temperature was obtained as follows [31].

$$\log D = -\frac{E_d}{2.303RT} + \log D_0 \quad (3)$$

where E_d is the diffusion activation energy of the inclusion compound, and D_0 is the diffusion coefficient of the inclusion compound at infinite temperature. A linear fit of log$D$ to the reciprocal of temperature produced a straight line ($R^2 = 0.9940$). The straight line is shown in Fig. S6B (Supporting information); moreover, E_d was calculated as 37.36 kJ/mol.

Cur toxicity affects unhealthy cells through membrane-mediated mechanisms, and usually exhibits lower cytotoxicity against normal cells than traditional chemotherapeutic drugs [47]. Despite these attractive properties, the use of pure Cur in cancer therapy is still restricted owing to its low bioavailability and solubility under physiological conditions. In the following study, the host–guest strategy was selected to embed Cur in a water-soluble polymeric matrix, which could efficiently control the release of Cur and increase its bioavailability.

To determine the cytotoxic potential of Cur-β-CDP, HepG2 cells were incubated with various concentrations of Cur, β-CDP, and Cur-β-CDP for 24 h, which was followed by evaluation of cell viability *via* MTT assay. The results of the cytotoxic effects against HepG2 are shown in Fig. 3A. Overall, β-CDP was almost non-toxic to HepG2 cells at concentrations of 5–80 μmol/mL, indicating that β-CDP could be a potential pharmaceutical carrier [48]. Both pure Cur and Cur-β-CDP showed cytotoxic effects on HepG2 cells, thereby verifying the anti-cancer activity of Cur-β-CDP resulting from released Cur. The viability of HepG2 cells decreased from 94.04% to 51.98% with increasing concentrations of Cur ranging from 5 μmol/mL to 80 μmol/mL. In parallel, the viability of HepG2 cells decreased from 91.94% to 44.81% with increasing concentrations of Cur-β-CDP. The results indicate that the Cur inclusion complex exhibited stronger inhibitory effects on HepG2 cells than Cur. In addition, the IC_{50} values of Cur and the Cur-β-CDP complex were measured as 32 and 28 mg/L, respectively. These results demonstrated that host-guest complexation with β-CDP improved the bioavailability of Cur. And it indicated that Cur-β-CDP exhibited stronger inhibitory effects on HepG2 cells than Cur and Cur-pillar[5]arene [49].

The cellular morphological photos of the HepG2 cells with different concentrations of the inclusion complex (1–80 μmol/L) for 24 h were microscopically observed, as shown in Fig. S7 (Supporting information). With an increasing concentration of Cur-β-CDP, the number of cells decreased gradually, and the morphology of the cells became round compared to the control cells. This alteration was consistent with the detection of cell viability. It was clear that, for the inclusion complex, β-CDP served as a complexation

host to enhance the water solubility of Cur, and improved the anti-cancer activity of Cur.

The synergistic effect of the host–guest complexation between β-CDP and Cur prevented the proliferation of the liver cells. The formation of the inclusion complex could protect Cur against biological degradation, which was a relevant factor to ensure the cytotoxic effect of Cur on the cancer cells [50].

To further investigate the *in vitro* cell efficacy of Cur-β-CDP, Cur, β-CDP, and Cur-β-CDP were chosen to study cellular uptake *via* confocal fluorescence microscopy, wherein blue spots indicate the nuclei of HepG2 cells. Cur and Cur-β-CDP are shown in green, owing to the fluorescence of Cur. Moreover, β-CDP has no fluorescence. The HepG2 cells incubated with Cur-β-CDP displayed strong fluorescence, which was distributed over a large area of the cell, except for the nucleus, whereas the HepG2 cells incubated with Cur exhibited a slightly weaker fluorescence that was distributed in a smaller area of the cell, again except for the nucleus (Fig. 3B). This suggests both Cur and Cur-β-CDP are mainly distributed in the cytoplasm. Therefore, compared to Cur, the HepG2 cells absorbed more Cur-β-CDP. The phagocytic effect of Cur-β-CDP was slightly better than that of Cur, indicating the high-water solubility and drug absorption of Cur-β-CDP.

Cell migration contributes to the metastasis of malignant tumors, leading to a poor prognosis for cancer patients. We performed an *in vitro* wound healing assay to study cancer cell migration in response to mechanical scratch wounds. The wound healing process was followed by taking time-lapse images at 0, 24 and 48 h, as shown in Fig. 3C. The wound was 34.3% closed at 24 h and 63.8% closed at 48 h for untreated cells. The results show the effect of Cur, β-CDP, and Cur-β-CDP (percentage of healing rate after 24 h and 48 h respectively. The inhibitory effects of Cur and Cur-β-CDP on cell migration were almost the same. After 48 h, compared with Cur and β-CDP, Cur-β-CDP inhibited cell migration more strongly in Fig. S8 (Supporting information). This significantly inhibited the healing rate within 48 h. Thus, Cur-β-CDP can release Cur sustainably for long-term treatment of malignant tumors. These results show that Cur can be released from the Cur-β-CDP complex and inhibit tumor cell migration. The influence of Cur-β-CDP was even stronger within 48 h compared with Cur, indicating that Cur-β-CDP was stable and that Cur could be released sustainably.

In conclusion, we characterized the host–guest interactions between Cur and β-CDP using various methods. The dissociation constant of the Cur $\subset$ CD unit in β-CDP was calculated to be 6.4×10^{-3} mol/L and the binding stoichiometry was confirmed to be 1:1. The water solubility of the inclusion complex was much higher than that of pure Cur. The host–guest interaction of Cur-β-CDP in water was also studied *via* CV. The diffusion coefficients of the oxidized and reduced states were calculated as 7.94×10^{-8} and 9.91×10^{-8} cm^2/s, respectively. The diffusion activation energy was calculated as 37.36 kJ/mol. Notably, Cur could serve as an included guest molecule and as an anti-cancer agent, which could strengthen biomedical applications. Cur-β-CDP effectively inhibited the growth of HepG2 cells, while having little effect on non-tumor cells. Moreover, this study demonstrated a promising approach for the improvement of Cur drugs with low water solubility, by enhancing the solubility and improving their anti-cancer performance.

Declaration of competing interest

The authors declare that they have no known competing financial interests or personal relationships that could have appeared to influence the work reported in this paper.

Acknowledgments

This work was supported by the National Natural Science Foundation of China (Nos. 21703200 and 21773203), the Chey Institute for Advanced Studies International Scholar Exchange Fellowship for the Academic Year of 2021–2022, and China Scholarship Council Program (No. 201908320084).

Supplementary materials

Supplementary material associated with this article can be found, in the online version, at doi:10.1016/j.cclet.2021.12.037.

References

[1] Z. Stanić, Curcumin, Plant Foods Hum. Nutr. 72 (2017) 1–12.
[2] M.C. Fadus, C. Lau, J. Bikhchandani, H.T. Lynch, J. Tradit. Complement. Med. 7 (2017) 339–346.
[3] L. Chen, C. Hu, M. Hood, et al., Nutrients 12 (2020) 1193.
[4] Y. Xi, J. Ge, M. Wang, et al., ACS Nano 14 (2020) 2904–2916.
[5] D.N.K. Reddy, F.Y. Huang, S.P. Wang, R. Kumar, Curr. Pharm. Design 26 (2020) 5021–5029.
[6] M. Kharat, M. Skrzynski, E.A. Decker, D.J. McClements, Food Chem. 320 (2020) 126653.
[7] K. Jakubczyk, A. Drużga, J. Katarzyna, K. Skonieczna-Żydecka, Antioxidants 9 (2020) 1092.
[8] A. De, D.H. Beligala, T.M. Birkholz, M.E. Geusz, Integr. Cancer Ther. 18 (2019) 1–10.
[9] X.S. Wang, Z.R. Zhang, M.M. Zhang, et al., BMC Complement Altern. Med. 17 (2017) 412.
[10] M.K. Jeenger, S. Shrivastava, V.G. Yerra, et al., Nutrition 31 (2015) 276–282.
[11] M. Rai, R. Pandit, S. Gaikwad, et al., Nanotechnol. Rev. 4 (2015) 161–172.
[12] M. Moballegh Nasery, B. Abadi, D. Poormoghadam, et al., Molecules 25 (2020) 689.
[13] S. Afrin, F. Giampieri, M. Gasparrini, et al., Biotechnol. Adv. 38 (2020) 107322.
[14] Z. Ma, N. Wang, H. He, X. Tang, J. Control. Release 316 (2019) 359–380.
[15] M. Ghazaeian, K. Khorsandi, R. Hosseinzadeh, et al., J. Biomol. Struct. Dyn. 39 (2021) 6606–6616.
[16] R. Jamwal, J. Integrative Med. 16 (2018) 367–374.
[17] E.M.M. Del Valle, Process Biochem. 39 (2004) 1033–1046.
[18] T. Kuwabara, Y. Hosokawa, J. Hu, T. Ide, J. Incl. Phenom. Macrocycl. Chem. 93 (2019) 85–90.
[19] J. Wankar, N.G. Kotla, S. Gera, et al., Adv. Funct. Mater. 30 (2020) 1909049.
[20] P. de Vos, M.M. Faas, M. Spasojevic, J. Sikkema, Int. Dairy J. 20 (2010) 292–302.
[21] Y. Liu, D.E. Sameen, S. Ahmed, et al., Food Chem. 370 (2022) 131026.
[22] M.E. Davis, M.E. Brewster, Nat. Rev. Drug Discov. 3 (2004) 1023–1035.
[23] D. Jia, X. Ma, Y. Lu, et al., Chin. Chem. Lett. 32 (2021) 162–167.
[24] F. Madrid, M. Rubio-Bellido, E. Morillo, Sci. Total Environ. 715 (2020) 136986.
[25] G. Crini, Prog. Polym. Sci. 30 (2005) 38–70.
[26] Y. Zhou, J. Lu, Y. Zhou, Y. Liu, Environ. Pollut. 252 (2019) 352–365.
[27] A. Harada, Y. Takashima, H. Yamaguchi, Chem. Soc. Rev. 38 (2009) 875–882.
[28] C. Song, Y. Xiao, K. Li, et al., Chin. Chem. Lett. 30 (2019) 1249–1252.
[29] B. Tian, S. Hua, J. Liu, Carbohydr. Polym. 232 (2020) 115805.
[30] P. Jansook, N. Ogawa, T. Loftsson, Int. J. Pharm. 535 (2018) 272–284.
[31] W. Zhang, M. Chen, G. Diao, Electrochim. Acta 56 (2011) 5129–5136.
[32] B. Zhao, L. Jiang, Q. Jia, Chin. Chem. Lett. 33 (2022) 11–21.
[33] S. Zohrehvand, C.H. Evans, Polym. Int. 54 (2005) 744–753.
[34] B. Sun, Y. Tian, L. Chen, Z. Jin, Food Hydrocoll. 77 (2018) 911–920.
[35] C.A. Slabber, C.D. Grimmer, R.S. Robinson, J. Nat. Prod. 79 (2016) 2726–2730.
[36] F. Payton, P. Sandusky, W.L. Alworth, J. Nat. Prod. 70 (2007) 143–146.
[37] W. Zhang, M. Chen, X. Gong, G. Diao, Carbon 61 (2013) 154–163.
[38] V. Jahed, A. Zarrabi, A.K. Bordbar, M.S. Hafezi, Food Chem. 165 (2014) 241–246.
[39] C. Liu, W. Zhang, Q. Wang, et al., Org. Biomol. Chem. 11 (2013) 4993–4999.
[40] R. Wimmer, F.L. Aachmann, K.L. Larsen, S.B. Petersen, Carbohydr. Res. 337 (2002) 841–849.
[41] K.P. Sambasevam, S. Mohamad, N.M. Sarih, N.A. Ismail, Int. J. Mol. Sci. 14 (2013) 3671–3682.
[42] B. Tang, L. Ma, H.Y. Wang, G.Y. Zhang, J. Agric. Food Chem. 50 (2002) 1355–1361.
[43] W. Zhang, X. Gong, Y. Cai, et al., Carbohydr. Polym. 95 (2013) 366–370.
[44] E.J. Olson, P. Bühlmann, J. Org. Chem. 79 (2014) 830-830.
[45] K. Li, Y. Li, L. Yang, et al., Anal. Methods 6 (2014) 7801–7808.
[46] D.M. Wray, C. Batchelor-McAuley, R.G. Compton, Electroanalysis 24 (2012) 2244–2248.
[47] M. Montiel-Herrera, A. Gandini, F.M. Goycoolea, et al., Carbohydr. Polym. 128 (2015) 220–227.
[48] Y.Z. Chen, Y.K. Huang, Y. Chen, et al., Chin. Chem. Lett. 26 (2015) 909–913.
[49] F. Guo, T. Xia, P. Xiao, et al., Bioorg. Chem. 110 (2021) 104764.
[50] M.S. Gularte, R.F.N. Quadrado, N.S. Pedra, et al., Int. J. Biol. Macromol. 148 (2020) 140–152.